ELSEVIER

Coastal Engineering 43 (2001) 131–148

Coastal Engineering
An International Journal for Coastal, Harbour and Offshore Engineers

www.elsevier.com/locate/coastaleng

Energy balance of wind waves as a function of the bottom friction formulation

R. Padilla-Hernández *, J. Monbaliu

Hydraulics Laboratory, Katholieke Universiteit Leuven, Kasteelpark Arenberg 40, B-3001 Heverlee, Belgium

Received 4 September 2000; received in revised form 14 February 2001; accepted 15 March 2001

Abstract

Four different expressions for wave energy dissipation by bottom friction are intercompared. For this purpose, the SWAN wave model and the wave data set of Lake George (Australia) are used. Three formulations are already present in SWAN (ver. 40.01): the JONSWAP expression, the drag law friction model of Collins and the eddy–viscosity model of Madsen. The eddy–viscosity model of Weber was incorporated into the SWAN code. Using Collins' and Weber's expressions, the depth- and fetch-limited wave growth laws obtained in the nearly idealized situation of Lake George can be reproduced. The wave model has shown the best performance using the formulation of Weber. This formula has some advantages over the other formulations. The expression is based on theoretical and physical principles. The wave height and the peak frequency obtained from the SWAN runs using Weber's bottom friction expression are more consistent with the measurements. The formula of Weber should therefore be preferred when modelling waves in very shallow water.

Keywords: Waves; SWAN; Wave bottom friction; Lake George

1. Introduction

One of the main problems to advance our knowledge about how to model wind waves in very shallow water is lack of data from measurements. Contrary to the situation in deep water, the dynamics of waves in shallow water areas are dominated by their interaction with the bottom. The growth by wind, propagation, non-linear interactions, energy decay and possibly the enhancement of whitecapping, are all linked to how the waves interact with the bottom. To this respect, the wave measurements campaign in Lake George, Australia (Young and Verhagen, 1996. Hereafter YV) is as unique as the JONSWAP experiment (Hasselmann et al., 1973). The data obtained from the lake in water of limited depth provide a nearly idealized situation to test and analyze several of the most widely used bottom friction formulations.

There are different mechanisms for wave energy dissipation at the bottom, such as energy dissipation through percolation, friction, motion of a soft muddy bottom and bottom scattering. The relative strength of those mechanisms depends on the bottom conditions; type of sediment and the presence or absence of sand ripples, and on the dimensions of such ripples. It appears that the bottom friction is the most important mechanism for energy decay in sandy

* Corresponding author. Fax: +32-16-321-989.
E-mail address: roberto.padilla@bwk.kuleuven.ac.be (R. Padilla-Hernández).

0378-3839/01/$ - see front matter
PII: S0378-3839(01)00010-2

coastal regions (Shemdin et al., 1978). The energy decay by bottom friction has been a subject of investigation and a large number of dissipation models for bottom friction have been proposed since the pioneering paper of Putman and Johnson (1949). All those models reflect the divergence of opinions on how to model physical mechanisms present in the wave–bottom interaction process. One of the recent formulations proposed to simulate the wave energy dissipation by bottom friction is the eddy–viscosity model of Weber (1989). Investigating the effect of the bottom friction dissipation on the energy balance using several formulations, Luo and Monbaliu (1994) concluded that there was no evidence to determine which friction formulation performs best. The work presented here reflects the search for evidence.

To reach the objective, the numerical wave model SWAN was run with the bottom friction source term as 'unknown' in order to reproduce the Lake George measurements (YV) in the best possible way. Besides the three formulations already present in SWAN (Booij et al., 1999; Section 3.2), also the formulation for bottom friction formulation by Weber (1989) was used. To this end, it was introduced in the SWAN model code. Although all of the individual source term formulations are open to discussion, it is assumed that the SWAN model computes the energy balance as a whole correctly. By only analyzing the term of dissipation by bottom friction, an attempt is made to select a formulation to be used in depth-limited situations.

2. The SWAN wave model

The SWAN (Simulation of WAves in Nearshore areas) model is based on the action balance equation. The equation solved by the SWAN model reads

$$\frac{\partial N}{\partial t}+\frac{\partial}{\partial x}(c_x N)+\frac{\partial}{\partial y}(c_y N)+\frac{\partial}{\partial \sigma}(c_\sigma N)+\frac{\partial}{\partial \theta}(c_\theta N)=\frac{S_{\mathrm{tot}}}{\sigma} \quad (1)$$

where $N(\sigma,\theta)$ is the wave action density ($=F(\sigma,\theta)/\sigma$); F is the wave energy density; t is the time; σ is the relative frequency; θ is the wave direction; c_x, c_y, are the propagation velocities in geographical x-, y-space; and c_σ and c_θ are the propagation velocities in spectral space (frequency and directional space). The first term of Eq. (1) represents the local rate of change of action density in time. The second and third terms stand for propagation of action in geographical space. The fourth term expresses the shifting of action density in frequency space due to variations in depth and currents. And the fifth term reproduces depth-induced and current-induced refraction. The source term $S(=S(\sigma,\theta))$ at the right-hand side of the action balance equation accounts for the effects of generation, dissipation and nonlinear wave–wave interactions. More explicitly, the source terms in SWAN include wave energy growth by wind input S_{in}; wave energy transfer due to wave–wave non-linear interactions S_{nl} (both quadruplets and triads); decay of wave energy due to whitecapping S_{ds}; bottom friction S_{bf}; and depth-induced wave breaking S_{bk}.

A detailed description of the SWAN (Cycle 2) model, the incorporated source terms and the numerical solution method can be found in Ris (1997), Holthuijsen et al. (1999) and Booij et al. (1999).

3. The models of bottom friction dissipation

3.1. Dissipation of wave energy as a function of bottom stress

Komen et al. (1994) start with the linearized momentum equation for the bottom boundary layer flow which in the case of pure wave motion (without ambient currents) reads

$$\frac{\partial \boldsymbol{u}}{\partial t}+\frac{1}{\rho}\nabla p=\frac{1}{\rho}\frac{\partial \boldsymbol{\tau}}{\partial z} \quad (2)$$

where t is time, z is the vertical coordinate, ρ is the density of the water, $\boldsymbol{u}$ and p the Reynolds-average horizontal velocity and pressure, respectively, and $\boldsymbol{\tau}$ the turbulent stress in the wave boundary layer. They obtain an expression for the wave energy dissipation due to bottom friction:

$$S_{\mathrm{bf}}(\boldsymbol{k})=-\frac{1}{g}\left\langle\frac{\boldsymbol{\tau}}{\rho}\cdot U_k\right\rangle \quad (3)$$

where the bottom friction depends on the known free orbital velocity (U_k) of the waves at the bottom and

on the unknown turbulent bottom stress ($\boldsymbol{\tau}$); the subscript k denotes a given wave number.

An exact solution for $\boldsymbol{\tau}$ in Eq. (2) (and hence for $S_{bf}(\boldsymbol{k})$ in Eq. (3)) does not exist, not even for a simple flow. To overcome the problem, several approaches have been proposed. Most of the approaches result in a turbulent shear stress expressed as a function of a friction coefficient and of a free-stream orbital velocity (orbital velocity at the top of the boundary layer). There are two distinct formulations for $\boldsymbol{\tau}$; the first is to retain a spectral description. The second is to represent the range of frequencies by a single frequency, for example, the peak frequency, resulting in an integral form.

Usually, $\boldsymbol{\tau}$ is expressed in a drag law as $\boldsymbol{\tau} = 1/2\rho C_D\ |\mathbf{U}|\mathbf{U}$ or, alternatively, as $\boldsymbol{\tau} = 1/2\rho C_D (U)_{rms}\mathbf{U}$, where C_D is a drag coefficient, $\mathbf{U}$ is the wave orbital velocity at the bottom and U_{rms} is the root mean square of the orbital velocity. Taking $C_f = 1/2 C_D\ |\mathbf{U}|$ or in the alternative expression $C_f = 1/2 C_D (U)_{rms}$ results in

$$\boldsymbol{\tau} = \rho C_f \mathbf{U} \tag{4}$$

Substitution of Eq. (4) in the dissipation Eq. (3) yields for every wave component with wavenumber $\boldsymbol{k}$:

$$S_{bf}(\boldsymbol{k}) = -\frac{1}{g} C_f \left\langle (U_k)^2 \right\rangle \tag{5}$$

The mean square of the bottom velocity, $\langle (U_{\boldsymbol{k}})^2 \rangle$, can be associated with the wave component having the wavenumber $\boldsymbol{k}$. Rewriting the expression (5) in terms of the wave spectrum, one obtains:

$$S_{bf}(\boldsymbol{k}) = -2C_f \frac{k}{\sinh 2kh} F(\boldsymbol{k}) \tag{6}$$

or equivalently (as expressed in SWAN model)

$$S_{bf}(\sigma,\theta) = -\frac{C_f}{g} \frac{\sigma^2}{\sinh^2 kh} F(\sigma,\theta) \tag{7}$$

where C_f is a dissipation coefficient with the dimension in m s^{-1}, and $F(k)$ and $F(\sigma,\theta)$ are the energy–density spectrum in wavenumber-space or in frequency-direction space, respectively. The vector $\boldsymbol{k} = (k_1,\ k_2) = (\boldsymbol{k}\cos\theta,\ \boldsymbol{k}\sin\theta)$ is the wavenumber vector with modulus k and direction θ, and σ is the relative frequency. The different formulations for the bottom friction dissipation differ mainly in the expression given to the dissipation coefficient C_f.

Below, the expressions that are currently implemented in the SWAN model (version 40.01, Holthuijsen et al. 1999) as well as Weber's formulation for bottom friction dissipation are explained briefly.

3.2. Expressions for the dissipation coefficient C_f

3.2.1. The JONSWAP model

This is the simplest expression for bottom dissipation. It was proposed by Hasselmann et al. (1973). C_{fJ} is assumed to be constant and is given by

$$C_{fJ} = \frac{\Gamma}{g} \tag{8}$$

where g is the acceleration due to gravity. From the results of the JONSWAP experiment, they found a value for Γ of 0.038 m^2 s^{-3}. As long as a suitable value for Γ is chosen, this expression performs well in many different conditions. The value for Γ can be different for swell and for wind sea. Bouws and Komen (1983) found that the JONSWAP expression with a value of 0.038 m^2 s^{-3} for Γ yielded too low dissipation rates for depth-limited wind sea conditions in the North Sea. They selected a value of 0.067 m^2 s^{-3} in order to obtain a correct equilibrium solution for a steady state. The JONSWAP formulation is also implemented as the default friction formulation in the WAM model (Komen et al., 1994).

3.2.2. The Madsen model

Madsen et al. (1988) derived a bottom friction formulation based on the eddy–viscosity concept,

$$C_{fM} = \frac{f_w}{\sqrt{2}} \langle U^2 \rangle^{1/2} \tag{9}$$

where

$$\langle U^2 \rangle^{1/2} = \left[\int\int \frac{2gk}{\sinh 2kh} F(\sigma,\theta)\, d\sigma\, d\theta \right]^{1/2} \tag{10}$$

and f_w is a non-dimensional friction factor. In the SWAN model, the following formulation, based on the work of Jonsson (1966), for f_w is used:

$$f_w = 0.3 \qquad \text{for } \frac{a_b}{K_N} \le 1.57$$

$$\frac{1}{4\sqrt{f_w}} + \log_{10}\left[\frac{1}{4\sqrt{f_w}}\right] = m_f + \log_{10}\left[\frac{a_b}{K_N}\right] \qquad \text{for } \frac{a_b}{K_N} > 1.57 \tag{11}$$

where $m_f = -0.08$, a_b is a representative near-bottom excursion amplitude:

$$a_b = \left[2 \int\int \frac{1}{\sinh^2 kh} F(\sigma, \theta) \, d\sigma \, d\theta \right]^{\frac{1}{2}} \quad (12)$$

and K_N is the bottom roughness length. Graber and Madsen (1988) implemented the expression of Madsen in a parametric wind sea model for finite water depths.

3.2.3. The Collins model

Hasselmann and Collins (1968) derived a formulation for the bottom friction dissipation. They related the turbulent bottom stress to the external flow by means of a quadratic friction law. The dissipation coefficient they derived reads:

$$C_f = 2c \left\langle \delta_{ij} \langle U \rangle + \left\langle \frac{U_i U_j}{U} \right\rangle \right\rangle \quad (13)$$

where δ_{ij} is the Kroneker delta function; $\langle \ \rangle$ denotes the ensemble average, U is equal to $(U_1^2 + U_2^2)^{1/2}$, U_1 and U_2 are the near bottom orbital velocity components, and c is a drag coefficient determined experimentally as a function of the bottom roughness. Hasselmann and Collins proposed a value for c equal to 0.015.

Collins (1972) simplified the expression (13) for the dissipation coefficient by leaving out the dependence on the direction of the wave component and by using the total wave induced bottom velocity:

$$C_{fC} = 2c \langle U^2 \rangle^{\frac{1}{2}} \quad (14)$$

where $\langle U^2 \rangle$ can be computed from Eq. (10). Expression (14) is the one implemented in the SWAN model. The value of the drag coefficient c was set to 0.015. Cavaleri and Malanotte-Rizzoli (1981) implemented this friction model in a parametric wave model.

3.2.4. The Weber eddy–viscosity model

Weber's model for the spectral energy dissipation due to friction in the turbulent wave boundary layer is based on the eddy–viscosity concept. In this model, the turbulent shear stress is parameterized in analogy with the viscous stress, with the coefficient of molecular viscosity replaced by a turbulent eddy–viscosity coefficient.

Solving the Navier–Stokes equations in the turbulent boundary layer and using perturbation theory, Weber derived the following dissipation coefficient.

$$C_{fW} = u^* \{ T_k(\xi_0) + T_k^*(\xi_0) \}. \quad (15)$$

C_{fW} depends on the wave spectrum $F(k)$, the water depth h, and the bottom roughness K_N through the friction velocity u^*, and on the radian frequency ($\omega = 2\pi\sigma$) through ξ_0.

$$\xi_0 = \left(\frac{4(y_0 + h)\omega}{\kappa u^*} \right)^{\frac{1}{2}} = \left(\frac{4K_N \omega}{30 \kappa u^*} \right)^{\frac{1}{2}} \quad (16)$$

The variable ξ_0 reflects the ratio between the roughness length and the boundary layer thickness, which scales with u^*/ω; κ is the von Kármán constant set equal to 0.4; $(y_0 + h)$ is the theoretical bottom level and T_k is defined as

$$T_k(\xi_0) = -\frac{1}{2} \kappa \xi_0 \frac{Ker'(\xi_0) + iKei'(\xi_0)}{Ker(\xi_0) + iKei(\xi_0)} \quad (17)$$

T_k is a dimensionless complex function and depends on the radian frequency and thus on the wavenumber through the argument ξ_0. $Ker + iKei$ is the zero order Kelvin function (Abramowitz and Stegun, 1965). The prime denotes the derivative with respect to the argument ξ_0. Details of the derivation of the dissipation coefficient in the eddy–viscosity model are given in Weber (1989, 1991). It is of interest to look at the differences and similarities between the different formulations. The expression by Weber will be used here as the reference since it models explicitly the bottom friction dissipation mechanism.

The JONSWAP friction model does not interpret bottom dissipation in terms of a physical mechanism such as percolation, friction or bottom motion.

Weber's and Madsen's formulations differ in the fact that Madsen's model approximates the random wave field by an "equivalent" monochromatic wave. This approximation is applied at an early stage of their calculations. Therefore, Madsen's expression is only valid for a narrow, singled-peaked spectrum. In fact, Collins' drag-law dissipation expression is rederived. However, in the Madsen formulation the friction coefficient f_w depends explicitly on the wave field and on the roughness length.

The formula of Weber is able to compute the dissipation rate directly from the bottom roughness length through the stress parameterization. That offers the possibility to adapt the dissipation rate according to the changing roughness under different wave–current regimes. This could be important in some coastal areas. Moreover, the expression of Weber maintains the spectral description and can be applied to complex situations, where the wave field cannot be easily represented by one wave component (Weber, 1991).

4. Numerical experiments

4.1. Introduction

In the following numerical experiments, the goal is to analyze the performance of the bottom friction formulations of Hasselmann et al. (1973), the eddy–viscosity model of Madsen et al. (1988), the drag law turbulent friction model of Collins (1972) and the eddy–viscosity model of Weber (1989).

A comparison is made of SWAN model output with the data from the Lake George experiment (YV). The input files and the data for the SWAN runs are taken from case F41LAKGR of the "Suite 40.01.a of the bench mark tests for the shallow water wave model SWAN Cycle 2, version 40.01 (SBMSWAN)" (WL Delft Hydraulics, 1999).

4.2. Statistical analysis

In order to analyze the results from the SWAN model using the different bottom friction models by comparing them with measurements, a set of statistical parameters following Dingemans (1997) is used:

The bias. The difference between the mean of the observations (x_i) and the mean of the model results (y_i)

$$\text{Bias} = \overline{X} - \overline{Y} \tag{18}$$

where Mean $= \overline{X} = (\Sigma_i x_i/N)$, N is the number of data.

The rmse. The root mean square error

$$\text{rmse} = \left[\frac{1}{N}\sum_i (y_i - x_i)^2\right]^{\frac{1}{2}} \tag{19}$$

The si. The scatter index

$$\text{si} = \frac{\text{rmse}}{\sqrt{\overline{X}\overline{Y}}} \tag{20}$$

The re. The relative error or index of agreement

$$\text{re} = 1 - \frac{N \times \text{rmse}^2}{\text{pe}} = 1 - \frac{\sum_i |y_i - x_i|^2}{\sum_i \left(|y_i - \overline{X}| + |x_i - \overline{X}|\right)^2} \tag{21}$$

The relative error reflects the degree to which the observations are approached by the model results. Willmott (1981) introduced re as an index of agreement. (re = 1, for perfect agreement, normally $0 <$ re < 1). The parameter pe is known as the potential variance.

In the computations of the different statistical parameters, the imposed values of the wave parameters at the grid model boundary are not included in the analysis.

4.3. Lake George

4.3.1. Situation

The Lake George experiment represents nearly idealized wave growth in depth- and fetch-limited conditions. The lake is fairly shallow with a relative uniform bathymetry (depth about 2 m). It is approximately 20 km long and 10 km wide. A series of eight wave gauges were situated along the North–South axis of the lake (Fig. 1). The bottom is rather smooth (bottom ripples were practically absent) and the bottom material consists of fine clay (Ris, 1997). The wave measurements were carried out during the period from April 1992 until October 1993. Only data for which the wind speed and direction were relatively constant during the 30-min sampling period have been retained. The criteria used for this selection were that the wind speed should not vary by more than 10% nor should the wind direction turn by more than 10° to each side of the alignment of the instrument array (north/south) during the 30-min sampling period. (For a complete description see YV.)

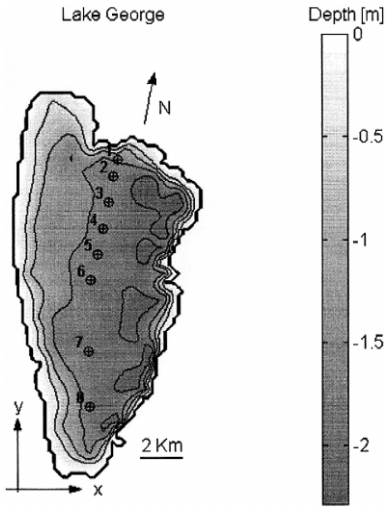

Fig. 1. Bathymetry of Lake George and the locations of the eight wave gauges. Depth contour interval is 0.5 m starting from 0.

For the computations, three northerly wind cases were selected from the bench mark data set for SWAN (SBMSWAN, case F41LAKGR). These cases are three typical examples, i.e., a low wind speed ($U_{10} = 6.5$ m s^{-1}), medium wind speed ($U_{10} = 10.8$ m s^{-1}) and a high wind speed ($U_{10} = 15.2$ m s^{-1}).

The computations were carried out with SWAN version 40.01 using the WAM Cycle 3 formulations (Booij et al., 1999). The wave–wave triad interactions and depth-induced wave breaking were turned on with default parameter values. For the bottom friction, one of the above formulations is used. As in Ris (1997), Station 1 is taken as the up-wave boundary in the simulation. This avoids uncertainty in the location of the northern shore because of seasonal variation in water depth. Since no directional wave spectrum is available at Station 1, the directional distribution of the waves is approximated with a $\cos^2(\theta)$ directional distribution. For the computations, a directional resolution of 10^0 and a logarithmic frequency resolution ($\Delta f = 0.1 f$) between 0.166 and 2.0 Hz for the low wind case and between 0.125 and 1.0 Hz for the medium and high wind case are chosen. The spatial resolution is 250 m both in x and y direction. To account for seasonal variations in water level, the water level was increased over the entire lake with $+0.1$, $+0.3$ and $+0.27$ m for the low, medium and high wind case, respectively.

4.3.2. Calibration

In order to tune the friction coefficients of every friction model, the third case (high wind speed) was chosen. The combined scatter index (sic) for H_s and T_p was taken as the cost function value to be minimized. The definition for the sic reads

$$\text{sic} = \left[\text{si}(H_s) + \text{si}(T_p)\right]/2 \qquad (22)$$

The results using the default value for the friction coefficient in every friction model is taken as a reference (see Table 1). An identical definition for the combined relative error (rec) is used, replacing re for si in Eq. (22).

The si for H_s and T_p and the sic are shown in Fig. 2. As can be observed in the figure, the behavior of the si is different for the different models. This figure shows how sensitive the wave parameters (H_s and T_p) are to variations in the friction coefficient in the case of the JONSWAP and the Collins expressions, and to variations in the roughness length, in the case of the Madsen and the Weber expressions.

For the JONSWAP formulation and starting from the default value, it is clear that lowering the value of the friction coefficient decreases the sic of H_s and T_p. The si of T_p reaches a minimum at a value of 0.030 m^2 s^{-3} for Γ. For an interval of Γ-values, the si of T_p is constant, but the results for H_s start

Table 1
Friction coefficient values for the different friction models and the resulting sic
The values in bold are the default and the underlined are the optimal values for the Lake George case.

Run No.	JONSWAP		Madsen		Collins		Weber	
	Γ	sic	K_N [mm]	sic	c	sic	K_N [mm]	sic
1	0.005	0.105	0.10	0.091	0.0005	0.120	0.01	0.079
2	0.010	0.090	0.25	0.090	0.0025	0.106	0.10	0.074
3	0.020	0.079	0.50	0.086	0.005	0.093	0.25	0.071
4	0.025	0.074	1.0	0.080	0.010	0.089	0.50	0.070
5	0.030	0.070	3.0	0.076	**0.015**	**0.081**	0.75	0.070
6	0.034	0.082	5.0	0.082	0.020	0.078	1.0	0.074
7	0.038	0.080	10.0	0.093	0.025	0.074	2.5	0.111
8	0.045	0.078	20.0	0.172	0.030	0.071	5.0	0.165
9	0.055	0.082	30.0	0.211	0.035	0.077	10.0	0.203
10	**0.067**	**0.092**	**50.0**	**0.214**	0.040	0.081	20.0	0.236
11	0.075	0.096	70.0	0.214	0.045	0.081	**40.0**	**0.241**
12	0.085	0.120	80.0	0.214	0.060	0.085	60.0	0.242

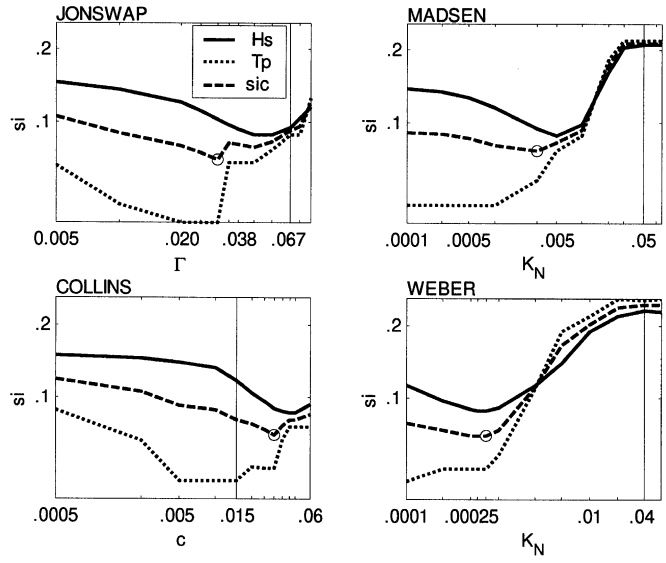

Fig. 2. The si for H_s and T_p, and sic in the function of the friction coefficient value in the Lake George case. The friction coefficient default value is indicated by a vertical line and the optimal value (the chosen value to run the three cases of Lake George) is indicated by a circle.

deteriorating. Nevertheless, lowering the value of Γ improves the sic about 23% compared with the results using the default value for Γ (see Table 1). The value retained for Γ is 0.030. It should be noted that the reference value for Γ was taken as 0.067, which is the appropriate value for depth-limited wind-sea case in the Southern North Sea (Bouws and Komen, 1983), and not as 0.038 which corresponds

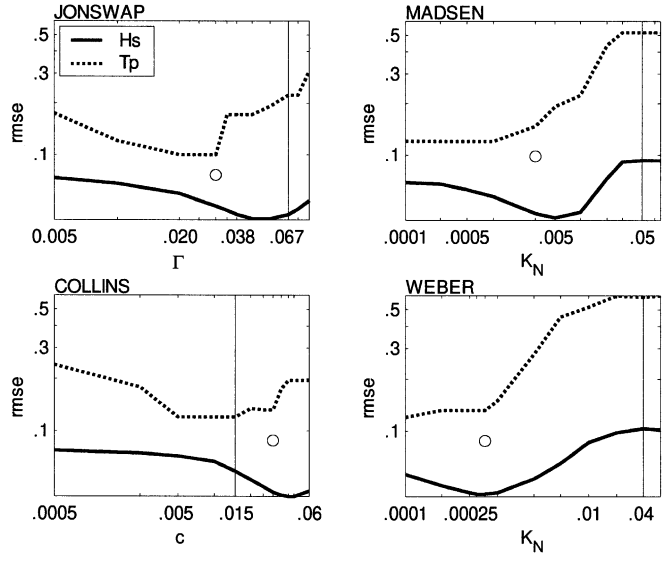

Fig. 3. Idem Fig. 2 but for rmse.

to swell conditions. The most suitable value for this case is even smaller than the value for swell conditions. The lowest value of the sic here corresponds with the lowest value of si for T_p.

Using the formulation of Madsen improvement of sic leads to improvement for both H_s and T_p. That is because both parameters H_s and T_p are underestimated using the reference value. The optimal value for K_N was chosen as 3×10^{-3} m. The improvement for the sic compared to the sic with the default value is about 64%. The lowest value of the sic does not correspond neither with the lowest value of the si for H_s nor with the lowest value of the si for T_p.

The sic varies little using the formulation of Collins for a region of c-values around the reference value. For higher than the reference value of c, the si for H_s improves but the si for T_p increases. Going to lower values of c, the si of both wave parameters increases. The value retained for c was taken equal to 0.030. According to Table 1 and Fig. 2, the sic has the best value but is only 14% different from the sic with the default c-value. The value retained for c, however, does neither produce the lowest value of the si for H_s nor for T_p. Looking at the rmse (Fig. 3) and the rec (Fig. 4), it is not so clear that the wave model gives the best results for a c-value equal to 0.030.

For the friction model of Weber, lowering the sic leads to improvement for both H_s and T_p. The changes of the si are rather smooth making the choice of the best value for K_N easy. The optimal value for K_N in Weber's formulation was chosen equal to 7.5×10^{-4} m. The improvement for the sic using the optimum value compared to the sic with the default value is about 71%.

Comparing the si, rmse and the re (Figs. 2, 3 and 4, respectively), the results using the formulation of Weber are more consistent in a statistical sense. The optimal value for K_N, according to the sic cost function, gives also the best value for the si, the rmse and the re for H_s. For T_p, the magnitude of those statistical parameters is quite close to the best values. That is not the case for the other formulations, especially not for the Collins' and Madsen's formulations. The lowest value for the sic (highest value of rec) does not correspond neither to the lowest si and rmse (highest re) for H_s nor to the lowest si and rmse (highest re) for T_p. As can be seen in Figs. 2, 3 and 4, the choice of the best value for the friction coefficient or the roughness length is prescribed mainly by the si of T_p. T_p is the parameter that improves most during the tuning process. Note that Ris et al. (1999) remarked that using the WAM cycle 3 formulations, SWAN systematically overestimates

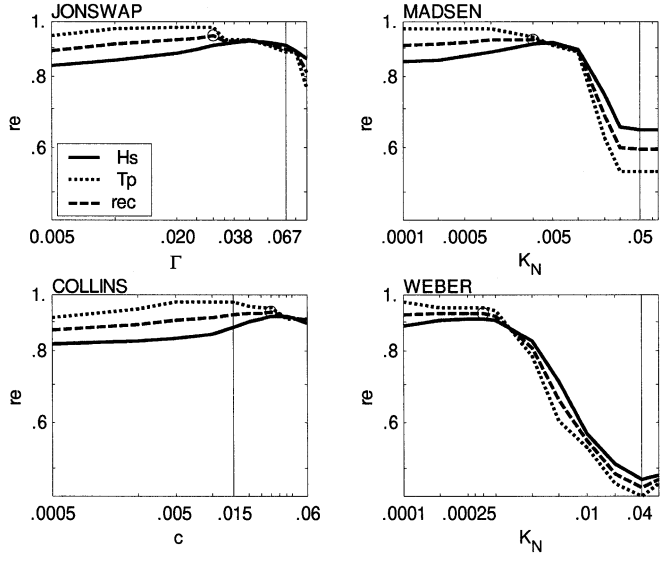

Fig. 4. Idem Fig. 2 but for the re and rec.

the significant wave height and underestimates the mean wave period.

It should be mentioned that a wave model run was made using a roughness length corresponding to the grain size at the bottom of the lake which is fine clay (Ris, 1997) of about $1.\times 10^{-6}$ m in diameter. The model was run using the expressions of Weber and Madsen. Comparing the results, using the expression of Weber, between the retained value for K_N (7.5×10^{-4} m) and the roughness length corresponding to the grain size ($1.\times 10^{-6}$ m) the sic increases by about 30%. The si for H_s increases by 54% and the si for T_p decreases by 12%. Using the Madsen expression with K_N equal to 1×10^{-6} m, the difference in the sic between the retained value for K_N (3×10^{-3} m) and the roughness length corresponding to the grain size (1×10^{-6} m) is about 38%. The si gets worse by 13% for T_p and by 55% for H_s. As can be seen from these results, even at very small values for K_N the dissipation by bottom friction still plays a role.

A wave model run without bottom friction for the case of high wind speed was made to see how important the bottom friction is. The value of the sic not considering the bottom friction is about 0.119. Comparing it with the value of 0.070, which is approximately the value of the sic using the optimal coefficients in the four bottom dissipation expressions (see Table 1), the difference is about 70%.

4.3.3. Validation

Once the appropriate values for the friction coefficients and roughness length were chosen (see Table 1, values underlined), the other two selected cases for Lake George were run using these values. It is assumed that the bottom condition did not change.

As can be see in Fig. 5, the significant wave height and the peak period are relatively well modeled by SWAN using either of the four friction models, except at the last three stations in case one. At these stations (from 6 to 8), the wave parameters do not show a monotonic behavior. That can possibly be ascribed to unresolved variation in the wind field. Such variation has been observed by YV. Those three stations were therefore eliminated from the statistical calculations for case one only. A small underestimation of T_p can be observed in the medium and low wind cases.

Fig. 6 shows the statistical parameters for the three wind cases for each of the four bottom friction

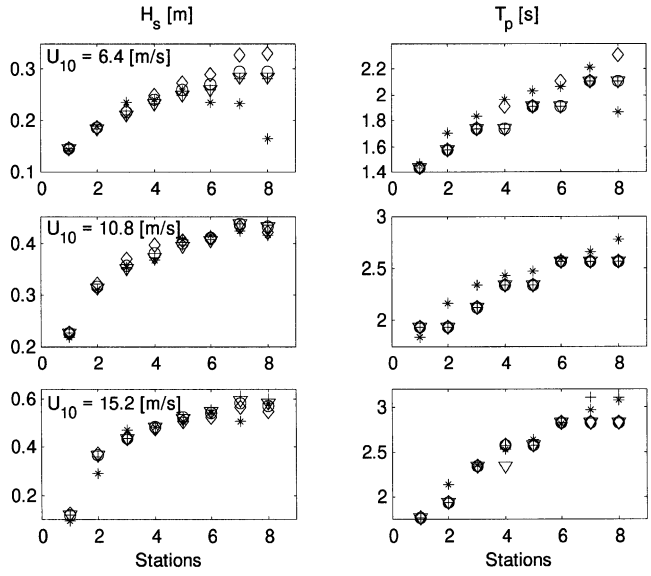

Fig. 5. SWAN model results for the different bottom friction formulations (with the optimal value for the friction coefficients) and observations of the significant wave height (left panels) and peak period (right panels) in nearly ideal generation conditions in Lake George. Observations (*), JONSWAP (+), Madsen (▽), Collins (○) and Weber (◇) formulations.

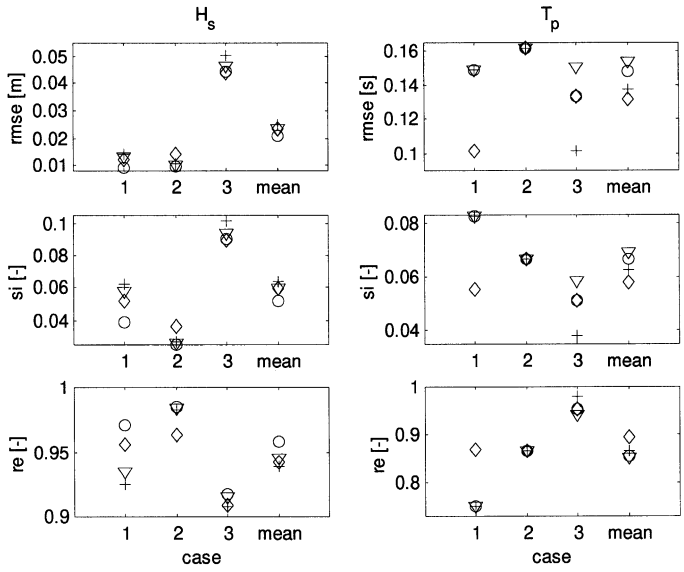

Fig. 6. rmse (top panels), si (middle panels) and re (bottom panels) for wave height (left panels) and peak period (right panels), for the three cases in Lake George. The "mean" case represents the mean value for the three cases. JONSWAP (+), Madsen (▽), Collins (○) and Weber (◇) formulations.

dissipation formulations used. The results from the SWAN runs are to a certain extent similar. The statistics show that using the formula of Collins, SWAN gives the best approximation for H_s but the approximation for T_p is not that good. From results, not shown here, using the default value for $c = 0.015$,

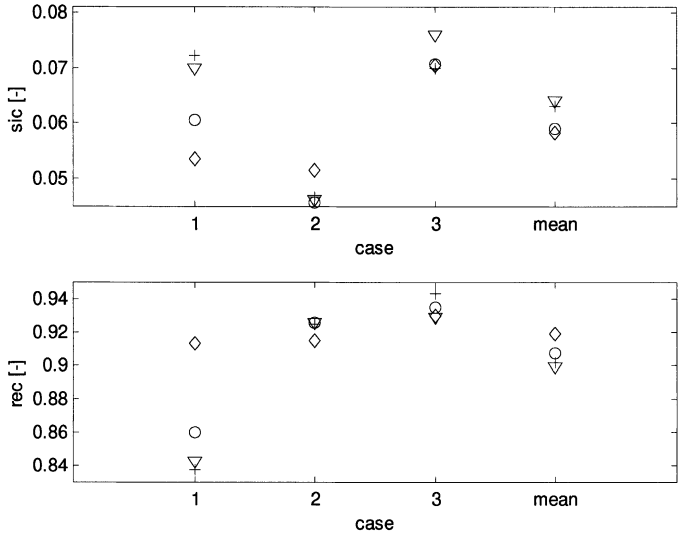

Fig. 7. Combined scatter index sic (top panel) and the combined relative error rec (bottom panel) for the wave height and the peak period. The "mean" case represents the mean values for the three cases. JONSWAP (+), Madsen (▽), Collins (○) and Weber (◇) formulations.

Table 2
Formulas for non-dimensional energy (ε) and non-dimensional frequency (ν) against non-dimensional depth, obtained from the results of SWAN using the different bottom friction models

Model	JONSWAP	Madsen	Collins	Weber
$\varepsilon =$	$4.1\times10^{-3}\ \delta^{1.76}$	$2.9\times10^{-3}\ \delta^{1.66}$	$1.4\times10^{-3}\ \delta^{1.42}$	$1.4\times10^{-3}\ \delta^{1.46}$
$\nu =$	$0.14\delta^{-0.472}$	$0.15\delta^{-0.430}$	$0.20\delta^{-0.375}$	$0.20\delta^{-0.375}$

C_{fC} gives the worst approximation for H_s but the best approximation for T_p.

Using the four bottom friction dissipation expressions, the largest error for H_s is in the high wind case compared with the other two cases. This can be partially ascribed to a 'deviation' of the measurements from the monotonic behavior in the locations 2 and 7 as can be seen in Fig. 5. Looking at the mean values of rmse, si and re for the three cases (Fig. 6), the best performance for H_s corresponds to the use of the Collins formulation and the best performance for T_p corresponds to the Weber formulation. Fig. 7 shows the performance of the SWAN using the different bottom friction formulations in the function of the combined statistics (sic and rec) of H_s and T_p. As can be seen, SWAN has the best performance using Weber's formulation followed by Collins, and then by the JONSWAP and the Madsen formulations. The peak period in the low wind case (for this wind field the bottom friction plays hardly any role) is very well reproduced using the formulation of Weber. This is not the case using the other formulations, as can be seen in Figs. 5 and 6.

4.3.4. Depth-limited wave growth

In order to refine the expressions of Bretschneider (1958) for both non-dimensional energy (ε) and non-dimensional peak frequency (ν), YV used their full data set of about 65,000 data points. They found that the asymptotic depth-limited growth can be considered dependent on the non-dimensional depth (δ) only. They found the following limits:

$$\varepsilon = 1.06\times10^{-3}\ \delta^{1.3} \quad (23)$$

$$\nu = 0.20\delta^{-0.375} \quad (24)$$

The non-dimensional parameters are defined as g^2E/U_{10}^4 for the non-dimensional energy (ε),

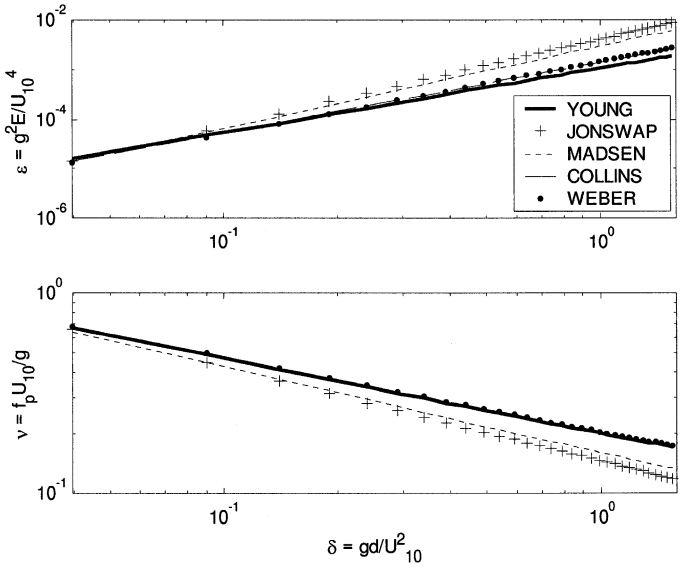

Fig. 8. Comparison of the SWAN results using the different bottom friction formulations and the formula from Young and Verhagen (1996) for non-dimensional energy ε (top panel) and non-dimensional peak frequency ν (bottom panel) against non-dimensional depth.

Table 3
Statistics comparing the values obtained from SWAN using the different friction formulations with the values according to the formulae from YV in the case of depth-limited growth

	Model	JONSWAP	Madsen	Collins	Weber
ε	bias	−0.002	−0.001	0.000	0.000
	rmse	0.003	0.002	0.000	0.000
	si	1.969	1.404	0.368	0.380
	re	0.800	0.816	0.955	0.953
ν	bias	0.055	0.055	0.000	0.000
	rmse	0.055	0.055	0.000	0.000
	si	0.243	0.241	0.000	0.000
	re	0.950	0.941	1.000	1.000

$f_p U_{10}/g$ for the non-dimensional peak frequency (ν), gd/U_{10}^2 for the non-dimensional depth (δ), g is the gravitational acceleration, E is the total energy of the spectrum, U_{10} is the wind speed measured at a reference height of 10 m, and d is the water depth.

To calculate the depth-limited growth, SWAN was run in one-dimensional mode for each of the friction models. Several runs were performed using different depths ranging from 2.5 to 20 m. The wind speed was set equal to 20 m s^{-1} (to work in the same non-dimensional depth interval as YV). The results were stored for different fetches ranging from 15 to 15,000 km. The friction coefficients and roughness length used have the optimal values retained from the tuning runs. The expressions given in Table 2 were computed taking the maximum levels of non-dimensional energy and the minimum non-dimensional peak frequency at every non-dimensional fetch of the different runs.

Fig. 8 shows the different retained results for ε and ν together with the expressions (23) and (24) of YV. Table 3 shows the statistics comparing them with the formulas obtained by YV. Although all of them give a good approximation to the measurements, it is clear that the formulae of Weber and Collins give the best results. The fit to the ν curve of YV is perfect. Because of the good approximation of all formulations to the formula from YV, Table 3 confirms that selecting sic as the parameter to be minimized was a good selection.

Even though YV considered that the asymptotic depth-limited energy growth depends on non-dimensional depth only, the numerical results show that the depth-limited growth is a function of the roughness length as well. If the bottom friction and bed material were not important in fetch- and depth-limited

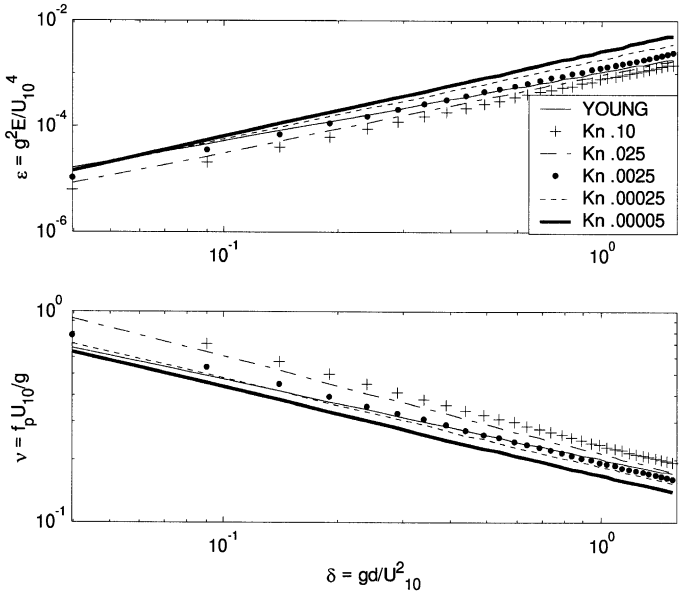

Fig. 9. Comparison of the SWAN results using the formulation of Weber with different roughness length (K_N) and the formula from Young and Verhagen (1996) for non-dimensional energy ε (top panel) and non-dimensional peak frequency ν (bottom panel) against non-dimensional depth.

conditions (as assumed by YV), then the value assigned to K_N should not matter and the results would be expected to be the same. This is not the case when the wave model is run using a different roughness length in the friction dissipation formulation. To exemplify this, the SWAN model was run for depth-limited wave growth with Weber's formulation for bottom friction. Fig. 9 shows the results for different values for K_N. Going from larger to smaller values of K_N, the ε increases and the ν decreases. Hence, one should expect that the curves for ε growth against non-dimensional fetch change as well. This implies that the expressions (23) and (24) should take into account the bottom roughness. The asymptotes for ε and ν can be expressed as:

$$\varepsilon = A\delta^{B} \tag{25}$$

$$\nu = C\delta^{D} \tag{26}$$

One can see from Fig. 9 that the roughness length has more influence on A and C than on B and D. Changing K_N from 0.10 to 5×10^{-5} m, A changes around 250%, B changes 8%. C and D change 30% and 9%, respectively. K_N has more impact on the energy than on the frequency. This suggests that A and C are functions of K_N.

4.3.5. Fetch-limited wave growth

Using their data from Lake George, YV proposed a generalized form to the shallow water limits for the growth of non-dimensional energy (ε) and non-dimensional peak frequency (ν) with non-dimensional fetch (χ)

$$\varepsilon = 3.64\times10^{-3}\left\{\tanh A_1 \tanh\left[\frac{B_1}{\tanh A_1}\right]\right\}^{n} \tag{27}$$

$$\nu = 0.133\left\{\tanh A_2 \tanh\left[\frac{B_2}{\tanh A_2}\right]\right\}^{m} \tag{28}$$

where

$$A_1 = 0.292^{1/n}\ \delta^{1.3/n} \tag{29}$$

$$B_1 = \left(4.396\times10^{-5}\right)^{1/n}\chi^{1/n} \tag{30}$$

and χ is the non-dimensional fetch. ($\chi = gx/U_{10}^2$), x is the distance and

$$A_2 = 1.505^{1/m}\ \delta^{-0.375/m} \tag{31}$$

$$B_2 = 16.391^{1/m}\ \chi^{-0.27/m} \tag{32}$$

The coefficients n and m control the rate of transition from "deep" to "depth limited" conditions. YV performed a non-linear least squares analysis on their selected data set to determine n and m. Their analysis yielded n equal to 1.74 and m equal to -0.37. Expressions (27) and (28) give a family of curves, one for each value of δ.

The results from SWAN are compared with the equations given by YV. Figs. 10 and 11 show the results from SWAN using the different bottom friction formulations for δ equal to 0.10 and 0.50, respectively. The deep water asymptotic forms of Eqs. (27) and (28) and the same equations but for shallow water (n equal to 1.74 and m equal to -0.37) are also shown. As can be seen from those figures, SWAN overestimates the total energy for very short χ. In particular, energy growth in the high frequency range (very short fetches) is usually overestimated by SWAN. This overestimation is observed systematically. According to Ris et al. (1999), the overestimation of energy at short fetches can be ascribed to the linear wave growth term of Cavaleri and Malanotte-Rizzoli (1981). But in this work, the linear growth term was not taken into account. Results from the wave model using the linear wave growth shows no relevant differences with the results without the linear growth term. The observed overestimation of energy should be ascribed to another reason. The search for such reason is beyond the scope of this work.

The SWAN runs with the formulations of Collins and Weber for bottom friction dissipation catch the asymptotic levels of ε and ν given by the expression of YV quite well, better than when using the expressions of JONSWAP and Madsen. But as can be seen in Fig. 11, the wave model reproduces better the levels of non-dimensional energy when using the expression of Weber than when using the expression of Collins.

To quantify the differences between the model results and the expression of YV for fetch-limited growth, the wave model was run for a range of

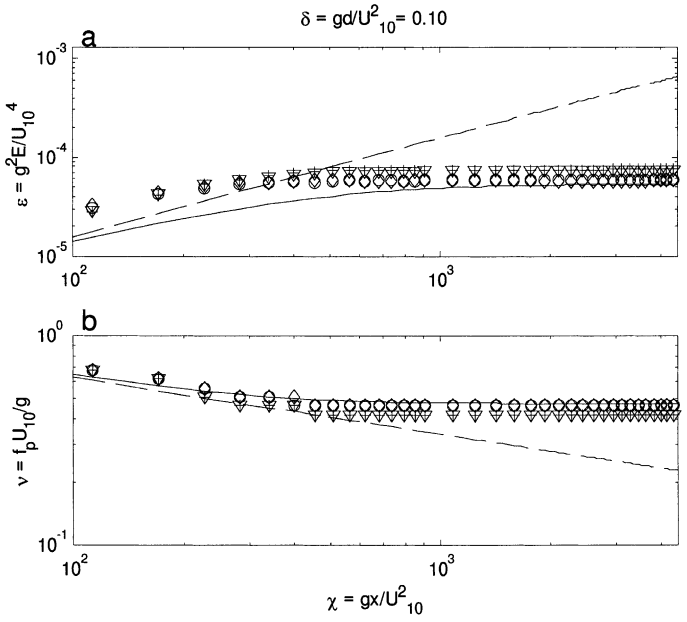

Fig. 10. (a) Non-dimensional energy ε and (b) non-dimensional peak frequency ν against non-dimensional fetch χ for a non-dimensional depth δ of 0.10. The deep water asymptotic form of Eqs. (20) and (23) is shown in dashed line. The same equations but for shallow water as found by YV ($n = 1.74$ and $m = -0.375$) is in solid line. SWAN was run using JONSWAP (+), Madsen ($\triangledown$), Collins ($\bigcirc$) and Weber ($\diamond$) formulation.

values of δ. The four statistical parameters given in Section 4.2 are computed.

Fig. 12 shows the statistical parameters comparing ε from the wave model results against the ε

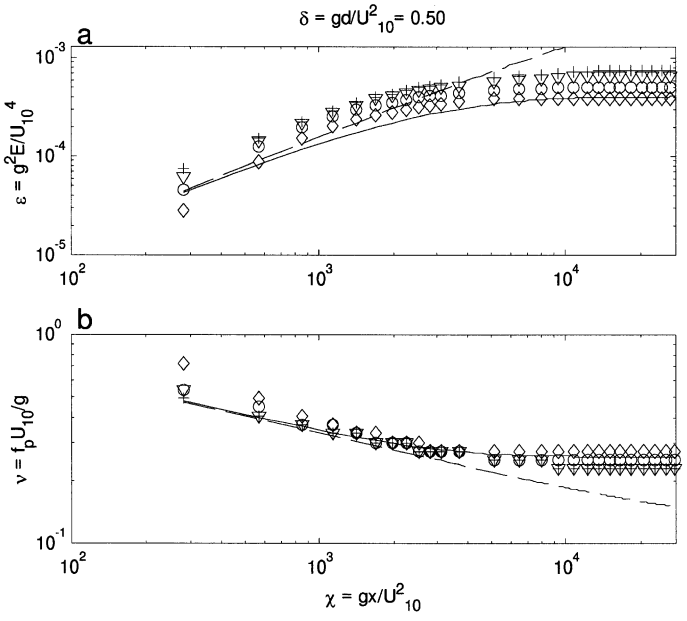

Fig. 11. Idem Fig. 10 but for a non-dimensional depth δ of 0.50. SWAN was run using JONSWAP (+), Madsen ($\bigcirc$), Collins (dotted) and Webers ($\diamond$) formulations.

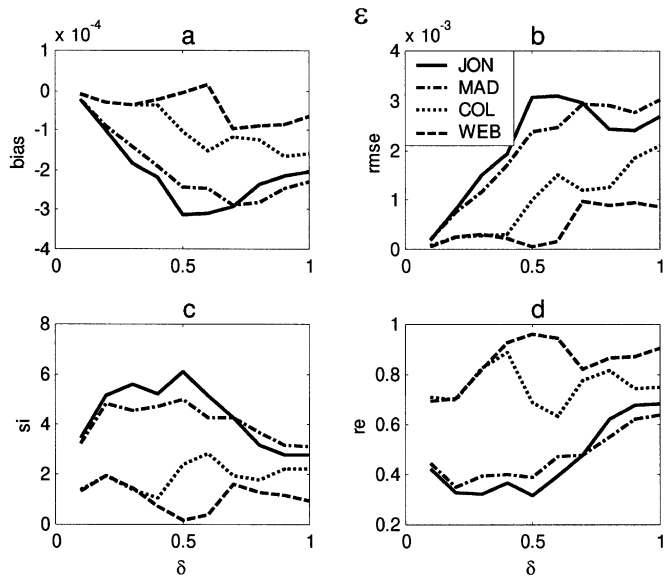

Fig. 12. The bias, rmse, si and re against non-dimensional depth δ. The comparison is done for wave growth in fetch-limited conditions between the non-dimensional energy ε from SWAN with the different bottom friction dissipation formulations and the formula from Young and Verhagen (1996).

computed from the YV expression (Eq. (27)) for a range of values of δ. Fig. 13 shows the same as Fig. 12 but for ν. In this way, Figs. 10 and 11 are represented statistically in Figs. 12 and 13 as two points at δ-values of 0.10 and 0.50, respectively. To calculate the fetch-limited growth, SWAN was run in one-dimensional mode for each of the friction models. Several runs were performed using a depth equal

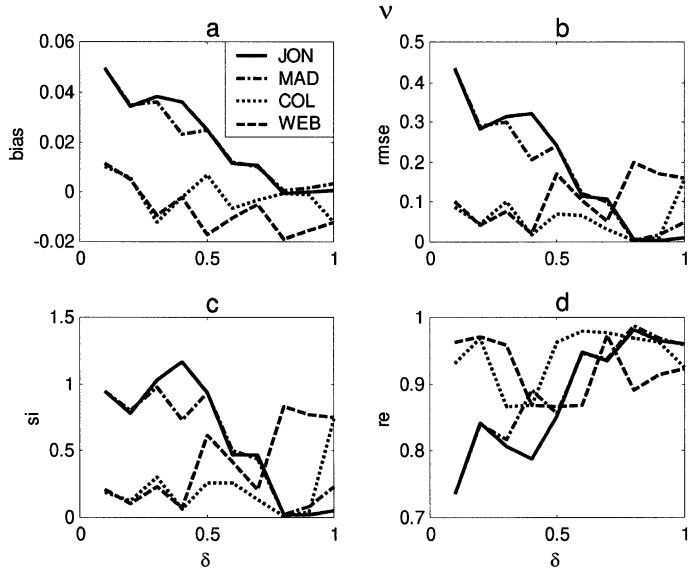

Fig. 13. Idem Fig. 12 but for non-dimensional frequency.

to 20 m and wind speed ranging from 10 to 31.3 m s^{-1} (to work in the non-dimensional depth range from 0.1 to 1.0). The total fetch for every run was 15,000 km with a resolution of 5 km. The fetch to compute the statistical parameters was different for every δ, depending on when the energy computed from Eq. (27) becomes constant (no changes in the seventh significant digit). The fetch range is from 440 km for δ equal to 0.1 to 997 km when δ is equal to 1.0. At small δ-values, SWAN gives results which have almost the same bias and rmse using either of the four bottom friction dissipation expressions. From Fig. 12a and b, it is evident that results start diverging going to deeper waters. At higher δ-values, the use of the expressions of JONSWAP and Madsen gives the largest bias and rmse. Applying the formulations of Collins and Weber, one obtains smaller bias and rmse, with a preference for Weber's expression. Looking at the four statistical parameters (Fig. 12), the results of SWAN using the formula of Weber approach better the non-dimensional energy ε computed by Eq. (27) and its behavior is more uniform along the non-dimensional depth axis, as can be seen in Fig. 12d.

Fig. 13 shows the statistics for the non-dimensional frequency ν of the SWAN results using the different bottom friction dissipation formulations. In contrast with ε, the bias and the rmse of ν do not have the same value for small δ. Contrary to the results for ε, the bias and the rmse decrease with increasing δ.

The statistical measures for ε indicate that using the expressions of Weber the wave model results approach quite well the values computed from Eq. (27), better than using the other three bottom friction formulations. With respect to ν, the wave results are of similar quality when the expressions of Collins and Weber are used and better than when using one of the other two expressions.

One can therefore conclude that in fetch- and depth-limited conditions, the computed wave parameters are more consistent when the bottom friction dissipation expression of Weber is used.

5. Summary and conclusions

The main objective was to investigate and clarify which bottom friction formulation performs best or is more consistent in shallow water regions. The SWAN model was run with the three formulations originally included plus the eddy–viscosity formulation of Weber. The data of Lake George were used to tune the friction coefficients of every formulation such that the combined scatter index was minimal. This exercise revealed different levels of difficulty in tuning the different friction coefficients.

Weber's model showed the best performance in the cases of depth- and fetch-limited wave growth. In the case of depth-limited wave growth, the fit of the calculated curve for the non-dimensional peak frequency to the one obtained by YV is as good as perfect. For the non-dimensional energy, the statistical values, rmse, si and re, show that the results using Weber's formulation are superior in approaching the equations obtained from YV. In the case of fetch-limited wave growth, the formulation of Weber showed the best performance in approaching the equations of YV derived from the measurements. Running the SWAN model using Weber's formula with different roughness length suggests that in the equations for depth- and fetch-limited wave growth the effect of bottom roughness should be included.

Formulations for dissipation by bottom friction, such as the model by Madsen or Weber, which take explicitly physical parameters for bottom roughness into account, should be preferred in wave modeling in shallow water areas. They offer the possibility to adapt the dissipation rate according to the changing roughness under different wave or wave–current conditions.

Besides showing the best performance, the formula of Weber has some other advantages. It was, at least for the Lake George case, easier to tune than the other formulations. The tuning parameter, namely, the bottom roughness length has a physical meaning. It gives information about the bottom boundary layer, through the friction velocity. It retains a spectral description making this formulation more reliable for a multi-modal wave spectra. It can be extended to the combined wave–current situation, important in situations where the tidal currents play a significant role in the dynamics of the coastal zone.

The above conclusions are based on two major assumptions. The first assumption states that the bottom friction dissipation is the only 'unknown' source term and the other source terms are repre-

sented correctly. The second assumption states that the conclusions would be the same if the bottom characteristics of the Lake George would, for example, change from fine clay to a sandy bottom. It would therefore be interesting to redo the above exercise when better formulations for the other source terms and/or when similar measurements but in a situation with a different bottom material become available.

Notation

a_b Near bottom excursion-amplitude [m]
c Coefficient in the Collins expression for the dissipation coefficient [–]
f_w Non-dimensional friction factor [–]
C_f Dissipation coefficient [ms^{-1}]
C_{fJ} JONSWAP dissipation coefficient [m s^{-1}]
C_{fM} Madsen dissipation coefficient [m s^{-1}]
C_{fC} Collins dissipation coefficient [m s^{-1}]
C_{fW} Weber dissipation coefficient [m s^{-1}]
c_x, c_y Wave propagation velocities in geographical x-, y-space [m s^{-1}]
c_σ, c_θ Wave propagation velocities in spectral σ-, θ-space [s^{-2}, rad s^{-1}]
d Water depth [m]
E Total energy of the wave spectrum [m^2]
f Frequency [Hz]
F Energy density spectrum [m^2 s rad^{-1}]
g Acceleration due to gravity [m s^{-2}]
h Total water depth [m]
H_s Significant wave height [m]
$\boldsymbol{k}$ Wavenumber vector [m^{-1}]
k Wavenumber [m^{-1}]
K_N Roughness length [m]
N Wave action density [m^2 s^2 rad^{-1}]
p Reynolds-average pressure [N m^{-2}]
re Relative error [–]
rec Combined relative error = (re(H_s) + re(T_p))/2 [–]
rmse Root mean square error [–]
S_{bf} Dissipation of wave energy by bottom friction [m^2 s rad^{-1}]
S_{bk} Dissipation due to depth-induced wave breaking [m^2 s rad^{-1}]
S_{ds} Dissipation by wave friction [m^2 s rad^{-1}]
S_{nl} Non-linear wave-wave interactions [m^2 s rad^{-1}]
si Scatter index [–]
sic Combined scatter index = (si(H_s) + si(T_p))/2 [–]
t Time [s]
T_p Wave peak period [s]
$\boldsymbol{u}$ Reynolds-average velocity [m s^{-1}]
u^* Friction velocity at the bottom [m s^{-1}]
U_k Orbital velocity at the bottom for a given wave number [m s^{-1}]
U_{10} Wind speed at 10 meters above the water level [m s^{-1}]
$\langle U^2 \rangle^{1/2}$ Root mean square of the orbital motion at the bottom [m s^{-1}]
x, y Horizontal coordinates [m]
z Vertical coordinate [m]
Γ Coefficient in C_{fJ} [m^2 s^{-3}]
δ Non-dimensional depth [–]
δ_{ij} Kronecker delta [–]
ε Non-dimensional energy [–]
θ Wave direction [rad]
κ von Karman constant [–]
ν Non-dimensional peak frequency [–]
ρ Density of the water [kg m^{-3}]
σ Relative frequency [rad]
$\boldsymbol{\tau}$ Turbulent stress in the wave boundary layer [N m^{-2}]
χ Non-dimensional fetch [–]
ω Radian frequency [rad s^{-1}]

Acknowledgements

R.P.H. gratefully acknowledges financial support from the Consejo Nacional de Ciencia y Tecnología (CONACYT, México). We also thank WL Delft Hydraulics for the SBMSWAN and Ian Young, University of New South Wales, Canberra, Australia, for the data of Lake George.

References

Abramowitz, M., Stegun, I.A., 1965. Handbook of Mathematical Functions. National Bureau of Standards, Washington, DC.

Booij, N., Ris, R.C., Holthuijsen, L.H., 1999. A third-generation wave model for coastal region: 1. Model description and validation. J. Geophys. Res. 104 (C4), 7649–7666.

Bouws, E., Komen, G.J., 1983. On the balance between growth

and dissipation in an extreme, depth limited wind-sea in the Southern North Sea. J. Phys. Oceanogr. 13, 1653–1658.

Bretschneider, C.L., 1958. Revised wave forecasting relationships. Proc. 6th Conference on Coastal Engineering, Gainesville/Palm Beach/Miami Beach, FL. ASCE, New York, pp. 30–67.

Cavaleri, L., Malanotte-Rizzoli, P., 1981. Wind wave prediction in shallow water: theory and application. J. Geophys. Res. 86-C11, 10961–10973.

Collins, J.I., 1972. Prediction of shallow water spectra. J. Geophys. Res. 93 (C1), 491–508.

Dingemans, M.W., 1997. Water Wave Propagation Over Uneven Bottoms: Part 1. Linear wave propagation. Advanced Series on Ocean Engineering, vol. 13, World Scientific, Singapore.

Graber, H.C., Madsen, O.S., 1988. A finite-depth wind wave model: 1. Model description. J. Phys. Oceanogr. 18, 1465–1483.

Hasselmann, K., Collins, J.I., 1968. Spectral dissipation of finite-depth gravity waves due to turbulent bottom friction. J. Mar. Res. 26 (1), 1–12.

Hasselmann, K., Barnett, T.P., Bouws, E., Carlson, H., Cartwright, D.E., Enke, K., Ewing, J.A., Gienapp, H., Hasselmann, D.E., Kruseman, P., Meerbrug, A., Müller, P., Olbers, D.J., Richter, K., Sell, W., Walden, H., 1973. Measurements of wind-wave growth and swell decay during the Joint North Sea Wave Project (JONSWAP). Dtsch. Hydrogr. Z., A 80 (12), 95 pp.

Holthuijsen, L.H., Booij, N., Ris, R.C., Haagsma, Ij.G., Kieftenburg, A.T.M.M., Padilla-Hernández, R., 1999. SWAN Cycle 2 version 40.01. User Manual. Delft University of Technology, The Netherlands.

Jonsson, I.G., 1966. Wave boundary layers and friction factors. Proc. 10th Int. Conf. Coastal Engineering. ASCE, Tokyo, Japan, pp. 127–148.

Komen, G.J., Cavaleri, L., Donelan, M., Hasselmann, K., Hasselmann, S., Janssen, P.A.E.M., 1994. Dynamics and Modelling of Ocean Waves. Cambridge Univ. Press, Cambridge, 532 pp.

Luo, W., Monbaliu, J., 1994. Effects of the bottom friction formulation on the energy balance for gravity waves in shallow water. J. Geophys. Res. 99 (C9), 18501–18511.

Madsen, O.S., Poon, Y.-K., Graber, H.C., 1988. Spectral wave attenuation by bottom friction: theory. Proc. 21st Int. Conf. on Coastal Eng. ASCE, Malaga, Spain, pp. 492–504.

Putman, J.A., Johnson, J.W., 1949. The dissipation of wave energy by bottom friction. Trans. Am. Geophys. Union 30, 67–74.

Ris, R.C., 1997. Spectral modelling of wind waves in coastal areas. PhD thesis. Delft University of Technology, The Netherlands.

Ris, R.C., Holthuijsen, L.H., Booij, N., 1999. A third-generation wave model for coastal region: 2. Verification. J. Geophys. Res. 104 (C4), 7667–7681.

Shemdin, P., Hasselmann, K., Hsiao, S.V., Herterich, K., 1978. Non-linear and linear bottom interaction effects in shallow water. Turbulent Fluxes Through the Sea Surface, Wave Dynamics and Prediction. NATO Conf. Ser. V, vol. 1, pp. 347–372.

Weber, S.L., 1989. Surface gravity waves and turbulent bottom friction. PhD thesis. University of Utrecht, the Netherlands.

Weber, N., 1991. Bottom friction for wind sea and swell in extreme depth-limited situations. J. Phys. Oceanogr. 21 (1), 149–172.

Willmott, C.J., 1981. On the validation of models. Phys. Geogr. 2 (2), 219–232.

WL Delft Hydraulics, 1999. SBMSWAN (Suite 40.01.a of the Benchmark Test for the Shallow Water Wave Model SWAN Cycle 2, version 40.01). Edited by Delft University of Technology.

Young, I.R., Verhagen, L.A., 1996. The growth of fetch limited waves in water of finite depth: Part 1. Total energy and peak frequency. Coastal Eng. 29, 47–78.